PLATFORM - A Journal of Engineering

Received: 17 April 2022, Accepted: 1 June 2022, Published: 30 June 2022, Publisher: UTP Press, Creative Commons: CC BY 4.0

STUDY OF THE PHYSICAL, MECHANICAL, CHEMICAL AND THERMAL CHARACTERISTICS OF PHENOLIC RESIN-STEEL SLAG REINFORCED COMPOSITES

Wasiu Ajibola Ayoola*, Chukwuemeka Oliver Onoh, Stephen Idowu Durowaye, Abdullah Abiodun Yusuf, Rasheed Olalekan Bankole, Elijah Oluwatosin Omoniyi, Abdulahi Akinkunmi Sanni

Department of Metallurgical and Materials Engineering, University of Lagos, Nigeria

*Email: wayoola@unilag.edu.ng

ABSTRACT

This study investigated the characteristics of non-asbestos brake pads in hybrid-polymer matrix composites. Steel slag, silica, calcium tri-oxocarbonate IV and graphite in varied weight percentages were added to the molten phenolic resin to develop the composites. The microstructural examination was carried out on the samples using a scanning electron microscope. The composites' physical, mechanical, chemical and thermal properties were evaluated at room temperature. The results obtained were compared with a commercial brake pad. The microstructure revealed a fair distribution of the particles in the resin matrix. The control sample exhibited the lowest wear rate of 0.6 and 0.8 g/Nm at loads of 7.5 and 10 N, respectively. This implies better wear resistance characteristics than the other samples. The samples exhibited appreciably high coefficient of friction of 0.410, 0.413, 0.440 and 0.40 for samples A, B, C and D, respectively, which is within the acceptable limit (0.3 – 0.6) for the brake pad. Sample A exhibited the highest compressive strength of 7.78 MPa, which is followed by samples C (3.04 MPa) and D (1.52 MPa). The results indicate that the compressibility of samples decreased with increasing steel slag and phenolic resin content. Sample D, which exhibited a lower wear rate (1 g/Nm) and coefficient of friction (0.40) than samples A, B, and C, exhibited the lowest water absorption rate. The specific gravity of the samples produced ranges between 2.45 and 2.61, which compare well with the commercial brake pad. Sample A was produced with the lowest proportion of steel slag and phenolic resin and exhibited the lowest acetone extraction. Samples A and B exhibited better thermal stability – an indication of good resistance to thermal decomposition. The thermal conductivity of the samples ranges between 134 and 193 W/mK, which is quite high compared to the standard and decreased significantly with an increase in temperature.

Keywords: *Hybrid polymer composites, steel slag, wear rate, coefficient of friction, compressive strength, thermal stability.*

INTRODUCTION

The brake system is one of the vital components of automobiles, without which driving safely will be impossible. Among the components of the braking system is the brake pad. The brake pad is used for speed reduction and stoppage of automobiles. It is a friction material, when pressed against the brake disc, dissipates the heat energy generated during braking application and dissipates the heat energy generated when pressed against the brake disc. The performance of a brake pad depends on its quality, and the rate depends on the type of materials used in the production of the brake pad. Brake pad composites contain binders, structural materials, fillers and frictional additives. Thus, materials selection is very important in developing friction materials because of the different characteristics that materials exhibit.

In service, brake pads are confronted with the problems of thermal decomposition and wear, which cause loss of friction and failure. The heat generated is absorbed by the friction materials (brake pads and rotors) before dissipating to the surroundings during braking [1]. The braking performance of automobiles can be affected significantly by the temperature rise in the brake components due to the frictional heat generated. High temperature during braking can cause brake fade, premature wear, brake fluid vapourisation, thermal cracks, and thermally excited vibration [1]. Hence, the need to develop non-carcinogenic brake pads that exhibit very high resistance to heat and wear. Many studies have been conducted on developing non-hazardous and durable brake pads for automobiles application using different kinds of materials. Asbestos-free brake pads were developed using sawdust to replace the use of asbestos, whose dust is carcinogenic. The sawdust was sieved into sieve grades of 100, 280, 355 µm, and 1 mm and used in the production of brake pad in the ratio of 20% resin, 10% graphite, 15% steel, 35-55% sawdust and 0-20% silicon carbide using compression moulding. The microstructure revealed uniform distribution of resin in sawdust. The results showed that the finer the sieve size, the better the properties. The properties exhibited by the composites in terms of density, water absorption, hardness, compressive strength, and flame resistance compared very well with that of commercial brake pads (asbestos-based and optimum formulation laboratory brake pad sawdust based) [2].

Asbestos-free brake pads were produced by compression moulding using agro waste-based cashew nut shells, Nigerian plant gum and other materials such as steel dust, graphite and silicon carbide. The cashew nut shells replaced asbestos for carcinogenic reasons, while the plant gum binder (Nigerian Gum Arabic) was used as a replacement for the toxic and commonly used epoxy resin binder. The composite exhibited hardness of 76.66 BHN, compressive strength of 17.197 N/mm^2, wear rate of 1.16 mg/m and coefficient of friction of 0.5632, which compared well with commercial asbestos-based brake pad [3].

Asbestos-free particulate ceramic matrix composites' thermal and tribological characteristics were investigated for possible application as an automobiles brake pad. Different formulations of the blend of 105-µm mill scale, 50-µm silica sand, 80-µm magnesia and 53-µm bentonite clay were used as input materials to develop particulate composites by powder metallurgy, and they were characterised. The composites exhibited high resistance to thermal decomposition in the temperature region of 0 – 1600°C, indicating thermal stability, appreciably high coefficient of friction (0.59) and a very low wear rate of 1.9093×10^{-6} g/m. The microstructure revealed a good dispersion and strong bonding of the particles in the microstructure, which enhanced the properties of the composites. These results are an indication that the composites are suitable for application in areas where high resistance to thermal stress and abrasive wear are required, such as the brake assembly of automobiles, specifically the brake pads [4].

The development of non-asbestos brake pads using composite materials to mitigate the challenge/problem of thermal decomposition and wear is imperative. Hence, this study aims to develop and characterise asbestos-free friction materials for application as automobile brake pads using phenolic resin (binder-matrix), steel slag (filler), silica (abrasive), graphite (lubricant), and calcium tri-oxocarbonate (IV) (reinforcement).

MATERIALS AND METHODS

Materials and Apparatus

The steel slag used for this study was obtained from African Steel Mills (Nig.) Limited Ikorodu, Lagos, Nigeria. The nominal chemical composition and phases present (Spectomax LM806-Amatek, USA) in the steel slag are shown in Tables 1 and 2, respectively. The phenolic resin, calcium trioxocarbonate IV ($CaCO_3$), and graphite were procured from a local vendor in Ojota Lagos, Nigeria. In addition, a commercial brake pad, optical vision microscope, DIN abrasive tester, Vickers hardness tester, weighing balance, hand

Table 1 Chemical composition of the steel dross used

Element	Al	Mg	Si	Mn	Fe	Ca	Na	Ti	P	S	K
(wt. %)	20.39	2.73	38.81	9.77	18.04	4.79	2.38	1.73	0.57	0.42	0.37

Table 2 Atomic concentration of the steel dross used obtained from XRD result

Phase	Al_2O_3	MgO	SiO_2	MnO	FeO	CaO	Na_2O	TiO_2	P	S	K
%	24.77	3.68	45.30	5.83	10.59	3.92	3.38	1.18	0.61	0.42	0.32

crusher and grinder, wooden mould, beakers, thread, stirring rod, metallic mortar and pestle were used. The commercial brake was purchased to benchmark the samples produced.

Materials Handling, Preparation and Production of Samples

The steel slag and silica were washed with distilled water and sundried to remove unwanted particles or dirt. They were then hand-crushed with a metallic mortar and pestle. Subsequently, both were ground and sieved with a 150 µm aperture. Figure 1 shows the as-received ground steel slag and silica. The yellowish-brown phenol-formaldehyde resin procured was in lump form. The $CaCO_3$ and graphite were in powdered form and used as-received except for pre-heating at 200°C to enhance the mixing homogeneity. The proportion of materials used in the formulation of experimental samples is shown in Table 3 using four different samples (A, B, C, and D). The materials itemised in Table 3 were mixed and poured inside a small crucible pot to produce the samples. The pot was covered and heated in a muffle furnace. The charge was held for approximately 10 minutes at 150°C with intermittent hand mixing for homogenisation of the mixtures. The holding temperature was measured using a hand-held thermometer. The homogenised mixtures were quickly poured into wooden moulds and immediately compressed for compaction. The samples were allowed to cool and cure for 24 hours before removing them. Before the characterisation of the models, they were allowed to cure for 10 days to allow for full curing. This process was used to produce all the composite and brake pad samples.

The same proportion presented in Table 3 was used in a preliminary study. Still, epoxy resin was used as the matrix instead of phenolic resin. This allowed for the samples' cold casting without any difficulty compressing the samples.

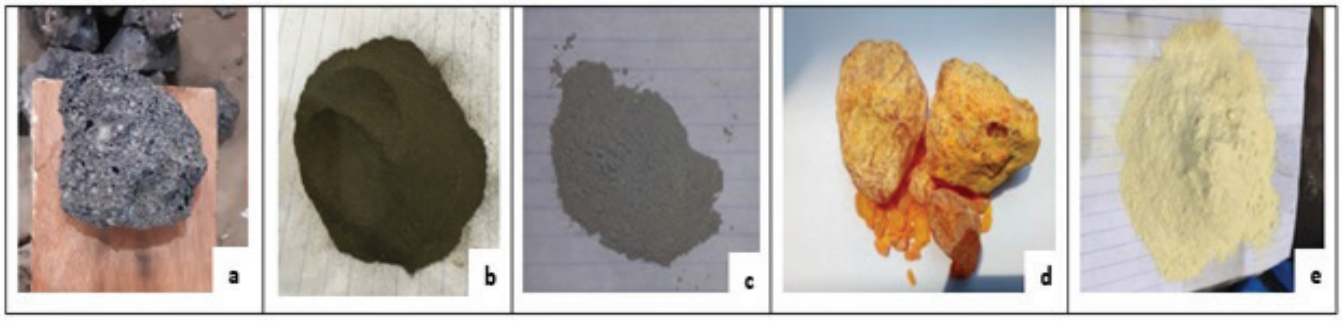

Figure 1 Photographs of raw materials used: (a) As-received steel slag, (b) ground steel slag, (c) ground silica, (d) phenolic resin lump and (e) ground phenolic resin

Table 3 The proportion of raw materials used to make the brake pads and their functions

Function	Materials % Mass (g)	Sample A	Sample B	Sample C	Sample D
		% Mass (g)	% Mass (g)	% Mass (g)	% Mass (g)
Binder	Phenolic resin	30	35	40	45
Reinforcement	$CaCO_3$	30	25	20	15
Filler	Steel slag	15	20	25	30
Abrasive	Silica	20	15	10	5
Lubricant	Graphite	5	5	5	5
Total		100	100	100	100

Characterisation of the Samples Produced Friction-Wear Test

The friction-wear test was carried out on a pin-on-disc tester (Model No: FE05000) equipped with a roller of length and diameter of 460 mm and 150 mm, respectively, and a torque of 40 rpm. Mesh emery paper P60 and abrasion distance 40 m were mounted on the pin-on-disc. Each as-cast samples was machined to 16 mm × 10 mm diameter. To ensure a uniform wear rate, each sample was placed at 100 mm diameter from the centre of emery paper during the test process. Separate emery paper was used for each test conducted. Before the wear test, the initial weight of the samples were taken and subsequently repeated after, with the aid of an electronic weighing balance to 0.01 mg accuracy. To avoid over-estimation, the worn-out pieces were thoroughly cleaned with wool soaked in acetone and wear particles removed. The difference between the initial weight and final weight was designated as mass loss, Δm. The wear rate was determined by [5]:

$$W = \frac{\Delta m}{L \times \rho} \quad (1)$$

where, W is wear rate (g/Nm), Δm is mass loss (mg), ρ is applied load (N) and L is a sliding distance (m).

Tensile Strength Test

Tensile test samples were prepared from the as-cast samples A, B, C and D with dimensions 250 × 25 × 10 mm and were conducted according to ASTM D3039 standard. The samples were subjected to a 10 kN load using an Instron universal tensile testing machine at a loading/crosshead speed of 30 mm/min (0.5 mm/s). As the sample stretches, the computer generates a graph and all the desired parameters until the sample fractures. The tester automatically plotted the graph of load against extension and various parameters of the sample determined are tensile strength, tensile strain, modulus, and tensile strain at break. The graph of load against extension was used to calculate the stress-strain relationship [6]. A simple sketch and photograph of the tensile test sample are shown in Figures 4b and 4c.

Compressibility Test

The compressibility test was conducted in accordance with ASTM D3410M standards. The same Instron universal tensile testing machine was used on the dimensions samples 135 mm × 25 mm × 10 mm at a loading/crosshead speed of 30 mm/min (0.5 mm/s). A load between 100 N and 10 kN was gradually applied and the corresponding strain was measured. The samples were subjected to compressive force, loaded continuously until failure occurred [7] and the load at which failure occurred was then recorded.

Water Absorption Test

The samples for the water absorption test were prepared and immersed in water in beakers shown in Figure 2. Before sample immersion, the initial weight of the sample was taken (W_1). The model was immersed in distilled water for 72 hours. The final weight of the sample (W_2) was also taken with a digital weighing balance that takes the readings up to approximately two decimal places. The % water absorption was calculated as [8]:

$$\%\ \text{Water Absorption} = \frac{W_2 - W_1}{W_1} \times 100\ \% \quad (2)$$

Specific Gravity Test

The ASTM D792 standards test method for specific gravity of plastic was used for the as-cast samples. The samples were weighed in air and water. The sample was immersed in water for 3 minutes and then weighed. The samples' specific gravity was calculated as [6]:

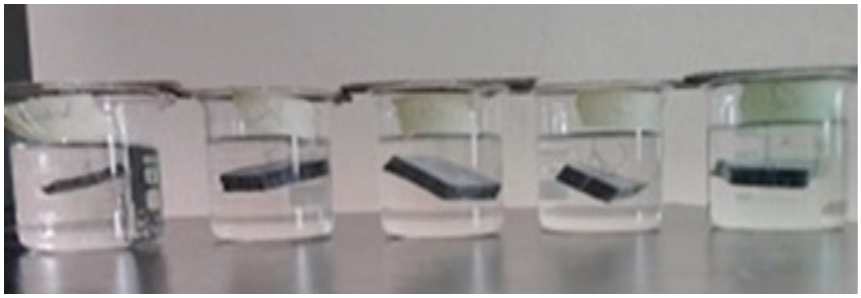

Figure 2 Experimental setup for water absorption test

$$\text{Specific Gravity (SG)} = \frac{W_a}{W_a - W_b} \times 100\ \% \qquad (3)$$

where, W_a is the weight (g) of sample in air and W_b is the weight (g) of sample in water.

Acetone Extraction

The materials and equipment used for the acetone extraction were Soxhlet apparatus, analytical weighing balance (accurate of 0.0001 g), 250 mm Whatman filter paper, 250 ml measuring cylinder and analytical grade acetone. The initial weight of the filter paper was taken as W_1, where 0.5 g of the sample was put on a filter paper and measured using a weighing balance. The weight was recorded as (W_2). The sample was placed in the Soxhlet flask and 200 ml of acetone was poured into it and was heated up to 56°C. The final weight was taken as W_3. The acetone extraction was obtained as given by [5]:

$$\%\ \text{Acetone weight} = \frac{W_2 - W_1}{W_3 - W_1} = \frac{\text{Weight of residue}}{\text{Weight of sample}} \times 100\ \% \qquad (4)$$

Thermal Conductivity

The thermal conductivity of the composite samples of 10 mm thickness and 10 mm diameter was determined according to ASTM C 1114-98 standard. The examples and commercial brake pads purchased were subjected to thermal conductivity tests at temperatures between 50 and 300°C [7],[9].

Thermogravimetric Analysis (TGA)

The thermogravimetric analysis of the samples was carried out according to the ASTM E2550 standard using a DTG 60 series type machine having an alumina pan of mass of 6.04 g. It was under a zero-air atmosphere (50 mL/min and the heating was at 10°C/min [6].

Scanning Electron Microscopy and X-Ray Diffraction (XRD)

Microstructural examination of the four formulations of the as-cast samples was conducted using a Scanning Electron Microscope (SEM) according to ASTM E766 standard. For the identification of the phases present in the control and experimental samples, an X-Ray Diffraction (XRD) analysis was conducted.

RESULTS AND DISCUSSION

Figure 3 shows the experimental samples (Figure 3a), and the produced brake pad sample (Figure 3b). The visual examination of the experimental samples A to D indicates that samples A and B appeared coarse while samples C and D looked fine, polished and darker. During the mixing of the proportion of materials used for the production of the samples, the percent mass of the graphite (lubricant) and silica (abrasive) was constant. However, the $CaCO_3$ (reinforcement), steel slag (filler), and phenolic resin (binding) materials that appeared dark were varied. The polish and dark appearances of the samples C and D were due to the decrease in percent proportions of the $CaCO_3$ on the one hand and an increase in the proportion of the steel slag and phenolic resin on the other hand - since no additional treatment was done on the samples. In the preliminary study, when the epoxy resin was used as the binder, a similar surface finish was seen (Figure 4). The preliminary study was abandoned/stopped because the samples failed during a minor driving test at a higher temperature due to the low melting point of epoxy resin used as the binder.

Wear and Frictional Characteristics

Figure 5 shows the results of the wear rate test conducted where two loads, 7.5 N and 10 N, were applied to the test samples. The wear rate of the samples varied with the formulation used. There is a decrease in wear rate with the addition of steel slag and phenolic resin. Sample A attained a wear rate of 1.25 and 1.67 g/Nm when loads of 7.5 and 10 N were applied. However, the significant effect of applied loads became lesser with samples C and D. Thus, the wear rate of sample D is less dependent on used. This trend suggests that the mass loss during wear is not always proportional to the applied load. The control sample exhibited higher wear resistance compared to the produced samples A to D, which could be due to the lack of proper compression of the samples after pouring [10]. The wear rate of the samples produced may be comparable to that of the control (commercial brake pad) when a hot press machine is used. The applied force was used to compound some charges where heat was removed from the spressurised charge, and the chemical reaction of the phenolic resin caused the hardening and wear resistance

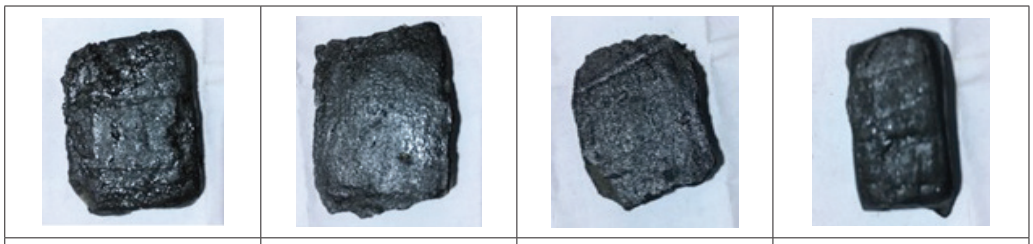

Sample A	Sample B	Sample C	Sample D

(a)

(b)

Figure 3 Photograph of the samples produced with phenolic resin (a) experimental samples and (b) sample of brake pad produced

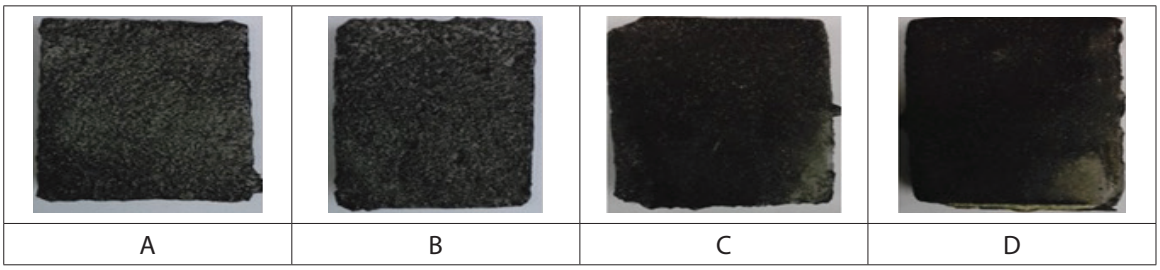

A	B	C	D

(a)

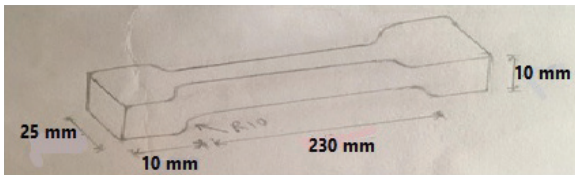

(b)

(c)

Figure 4 The test samples produced with epoxy resin: (a) visual appearance, (b) sketch and basic dimensions (c) overall appearance of the tensile test sample

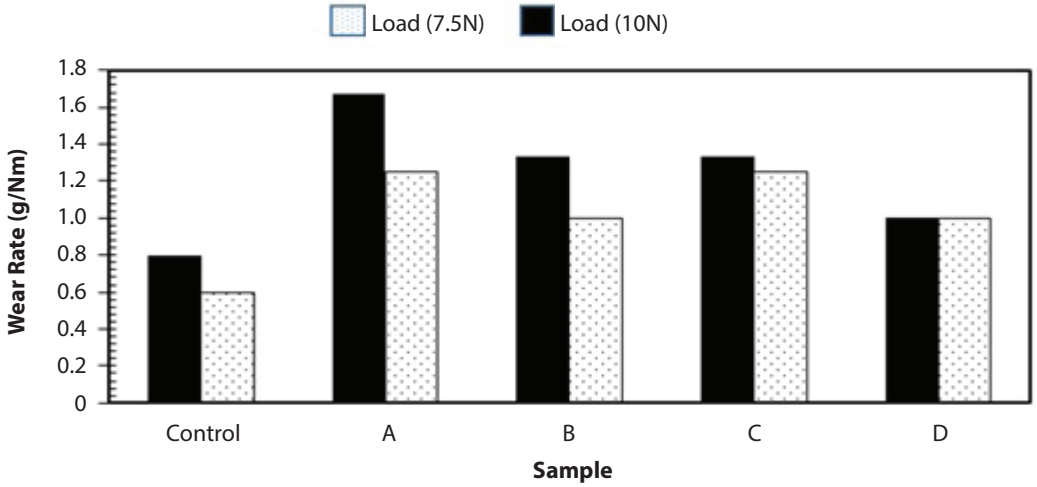

Figure 5 Wear rate of the control and as-cast samples

to increase [11]. The difference in the wear rate of the commercial brake pad and sample D is 25 %. Figure 5 also indicates that the wear rate decreased with increasing steel slag and phenolic resin addition (Table 3) since the wear resistance of a material is inversely proportional to the wear rate, sample D with the highest phenolic resin and steel slag proportion demonstrated the highest wear resistance.

The results presented indicate that phenolic resin and steel slag proportions enhanced the wear resistance of the samples. This is because steel slag and phenolic resin acted both as friction and abrasion resistance materials in the experimental samples. The two principal factors that affect the friction and wear resistance of samples are the chemical and physical properties of the materials. The chemical and physical properties of phenolic resin suggest that steel slag addition is more responsible for the wear behaviour [5].

Friction is an important property of a braking system, which requires adequate check and balance over a range of temperatures, speed and load [12]. End-users of brake pads expect pad friction to be stable and neutral to both the abrasive wear and adhesive wear and maintain the same frictional force level at various conditions [13]. Abrasive wear occurs due to the penetration and ploughing out of materials forming a surface of hard particles between the brake disc and brake pad. Adhesive wear occurs mainly in the high-temperature region [14]. The results of the coefficient of friction of the experimental samples A to D produced are shown in Figure 6. The average values of the three readings measured are 0.410, 0.413, 0.440 and 0.400 for samples A, B, C, and D. The

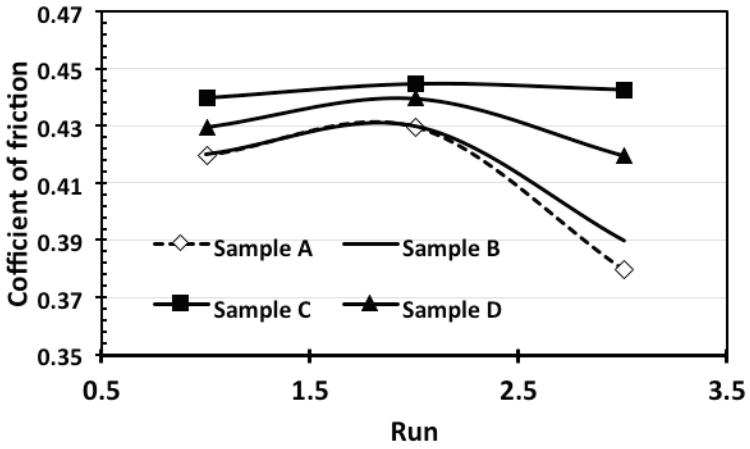

Figure 6 Coefficients of friction of samples A, B, C and D

samples exhibited an appreciably high coefficient of friction, which is within the acceptable limit (0.3 – 0.6) for the brake pad [15]-[16]. The deviation of the coefficient of friction of all samples is 9 %. This implies that the proportions of the materials selected for the production of the samples were appropriate for coefficient of friction property. The coefficient of friction of the commercial brake pad analysed is 0.54.

The stability observed in the coefficient of friction in the experimental samples could be due to the proper homogenisation of the constituents and adequate distribution of particles within the phenolic resin. It has been previously noted that steel fibres adversely increased the coefficient of friction which was attributed to the adhesion of metal chips [13]. Such behaviour was not observed due to the particulate form of the steel slag used.

Tensile Strength

Figure 7 shows the variation of the tensile and compressive strengths of the samples produced. In the figure, the compressive and tensile strengths increase with increasing tensile and compression strains, respectively. The tensile strength provides information on the level of pulling forces that a sample can absorb to break, while the compressive strength indicates the compression forces. The ultimate compressive (tensile) strengths of the samples A, B, C and D are as follows: 7.78 (1.43), 1.35 (2.00), 3.04 (0.19) and 1.52 (1.83) MPa, respectively. Sample A exhibited the highest compressive strength, which is followed by samples C and D. The results suggest that the compressibility of samples decreased with increasing steel slag and phenolic resin. This is because $CaCO_3$ and silica are ceramics of better compression strengths. The tensile strength is also shown in the figure. The addition of phenolic resin and steel slag did not significantly influence the tensile strength. The trend demonstrated is connected to the functions of phenolic resin and other constituents of the brake pad. Phenolic resin is a binder witha good combination of mechanical properties such as high hardness, high thermal resistance, compressive strength, and very good wetting capability with most of the materials and steel slag has better wear resistance and tensile strength. However, the results suggest a trade-off between the brake pad constituents that may achieve an optimum combination of ultimate compressive and tensile strengths. Increasing wt. % of phenolic resin and steel slag seems to enhance the tensile strength at the expense of compressive strength due to the type of phases present.

Water Absorption

Basically, water absorbed by brake pads is influenced by the amount and size of pores present. The presence of a high number of pores could lead to a low coefficient of friction and a high wear rate. Hence, the porosity level of brake pads should be low. Figure 8 shows the graph of water absorption of commercial

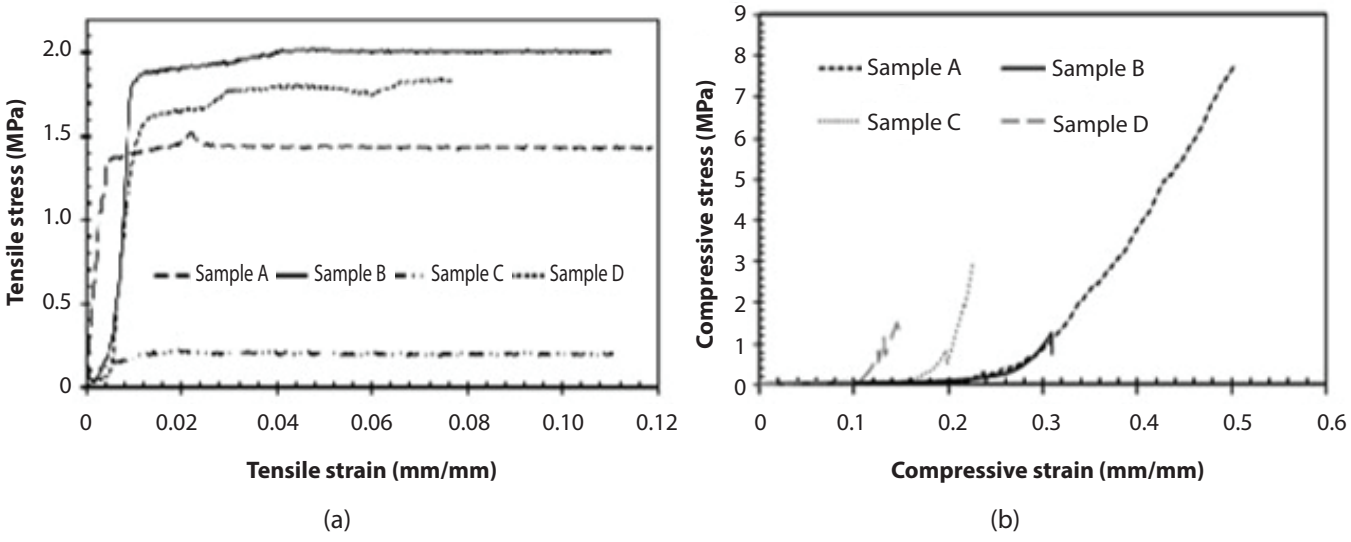

Figure 7 The stress-strain relationships of samples A, B, C and D: (a) tensile strength and (b) compressive strength

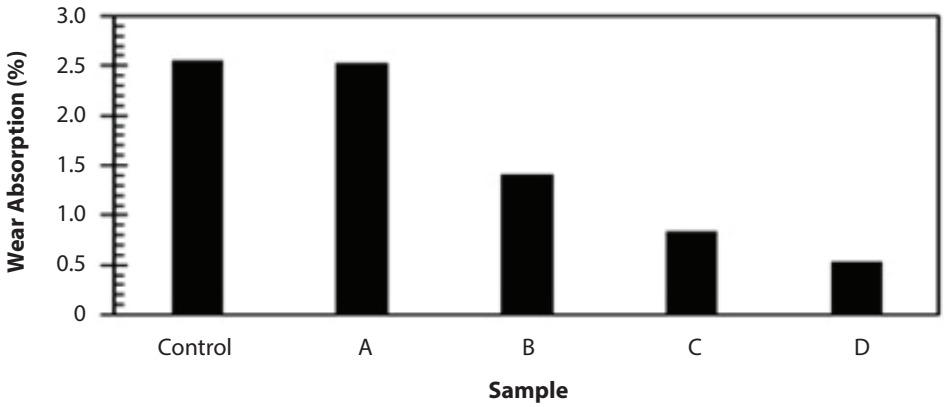

Figure 8 Water absorption of the commercial brake pad (control) and experimental samples produced

brake pad and experimental samples produced for different formulations presented in Table 3. From Figure 8, the water absorption level decreased from samples A to D, which translated to an increase in steel slag and phenolic resin. With the lowest wear rate and coefficient of 0.4, Sample D exhibited the lowest water absorption rate, which could be attributed to an increase in the density of the sample D [13]. The pores present decreased in volume with the addition of steel slag and phenolic resin, thereby increasing the density of the brake pads. The commercial brake pad (control) and sample A exhibited the same water absorption. This implies that the samples produced have superior water absorption properties over the commercial brake pad examined. At 72 hours of samples immersion in water, there was no further absorption indicating saturation by the samples.

Specific Gravity and Porosity

The specific gravity is the relative density of any given material, while porosity measures the void fraction in a material. Theoretically, materials with the highest specific gravity should exhibit the lowest porosity in comparison. Thus, specific gravity and porosity are physical properties that influence the thermal conductivity, strength, hardness, noise insulation, wear rate, friction coefficient and water absorption [17]. In Figure 9a, the specific gravity of the produced samples did not vary significantly with the different formulations of the constituents used. The specific gravity of the samples produced ranges between 2.45 and 2.61. The commercial brake pad has a specific gravity of 2.06, and the same value was reported for the commercial brake pad asbestos-based [13]. The values of specific gravity obtained agrees with the

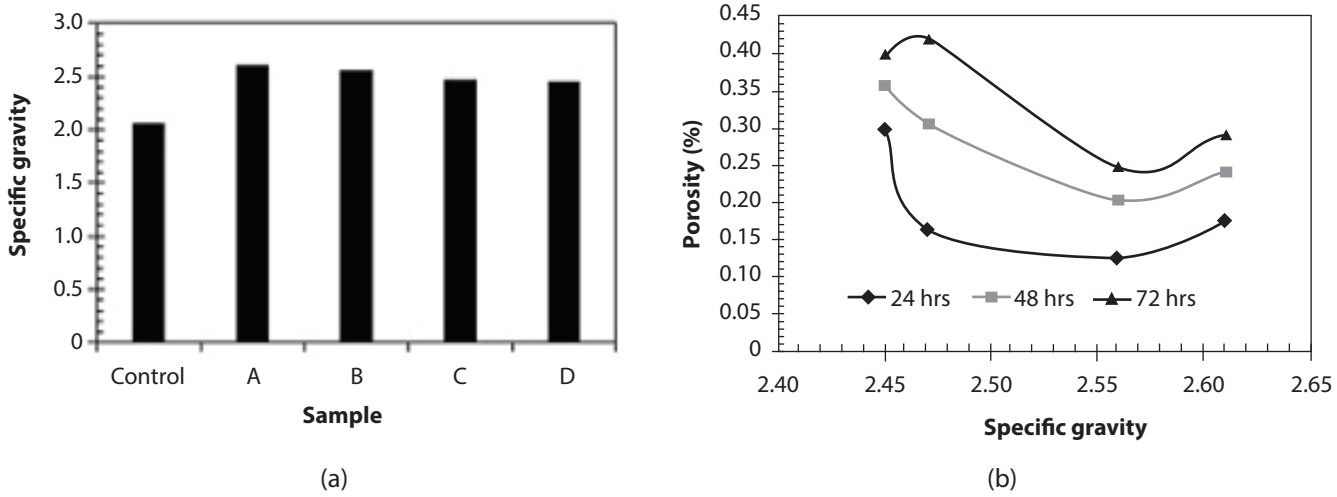

Figure 9 Physical properties of the samples: (a) Specific gravity values of the commercial brake pad and the sample and (b) the porosity as a function of specific gravity

values of 2.27 – 3.25 reported by Jaafar et al. [18] and compare well with the commercial brake pad.

Two methods are available to estimate the void fraction of brake pads as presented in Equations 5 and 6. Equation 5 is based on the rule of mixture. In previous studies, both Equations were used, and a similar trend was obtained [15]-[19]:

$$P_r = \left(1 - \frac{P_E}{P_T}\right) * 100\% \quad (5)$$

where P_r is the porosity (%), P_E is the experimental density (g/cm^3) and P_T is the theoretical density (g/cm^3).

$$P_r = \left(\frac{M_2 - M_1}{D}\right)\left(\frac{100}{V}\right) \quad (6)$$

In this study, Equation 6 was adopted for the estimation of porosity. Figure 9b shows the relationship between porosity and the specific density of the samples produced. The trend of the graphs indicates that porosity is increasing with decreasing specific gravity. Such a trend translates to increasing steel slag and phenolic resin. Factors that affect the density and porosity of brake pads are the sieve sizes of the constituents used, the individual density of the constituents, and homogeneity ensured during mixing, pressure and temperature [15].

Acetone Extraction

Figure 10 shows the graphs of acetone extraction of the commercial brake pad and produced samples for a different proportion of brake pad materials. Sample A was produced with the lowest proportion of steel slag phenolic resin and exhibited the lowest acetone extraction, which could be because of the higher per cent proportion of steel slag and, more importantly, the phenolic resin that experienced chemical reaction [20]. Hence, sample A exhibited better thermal stability and acetone extraction.

Thermo-Gravimetric Analysis

Figure 11 shows the Thermo-Gravimetric Analysis (TGA) graphs of loss of ignition of experimental samples and commercial brake pad. Clearly, from the graphs, the experimental samples started losing their weight at 200°C, which may be due to the thermal decomposition of phenolic resin or organic components present in the steel slag. The loss of weight on the ignition of the samples produced is superior compared to that of the commercial brake pad. Samples A and B have a closer loss of ignition weight and similarly for samples C and D. The loss of weight on ignition of the produced samples ranged between 3% and 20% when the temperature was between 150°C and 1300°C. The commercial brake pad exhibited weight loss on ignition of 70% at a temperature above 350°C. Samples A and B produced with a lower proportion of steel slag and phenolic resin exhibited the lowest loss weight on ignition (Figure 11a), which could be attributed to the higher percent proportion of $CaCO_3$ and silica. They both exhibited high thermal stability compared to the phenolic resin and steel slag. Oxidation and thermal decomposition of phenolic resin started above 300°C. Decomposition occurs between 300°C and 600°C where mainly gaseous components are emitted. Above 600°C, more materials and gases were released [21]-[22]. Hence, samples A and B exhibited better

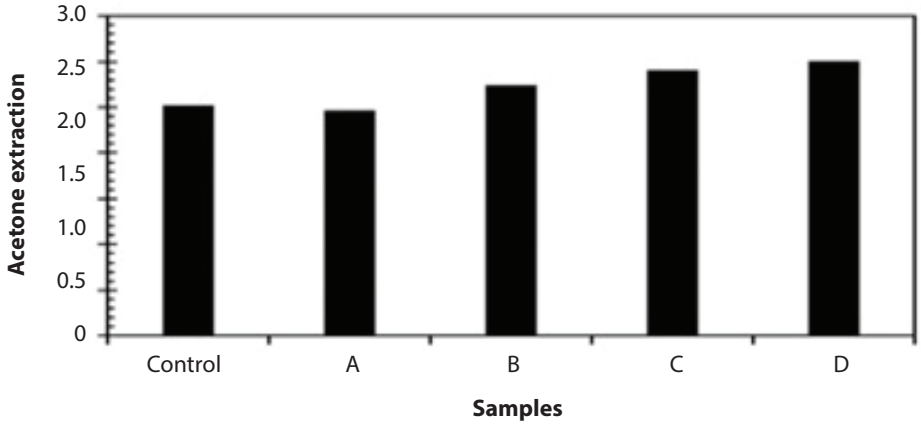

Figure 10 Acetone extraction for a different formulation of brake pad materials

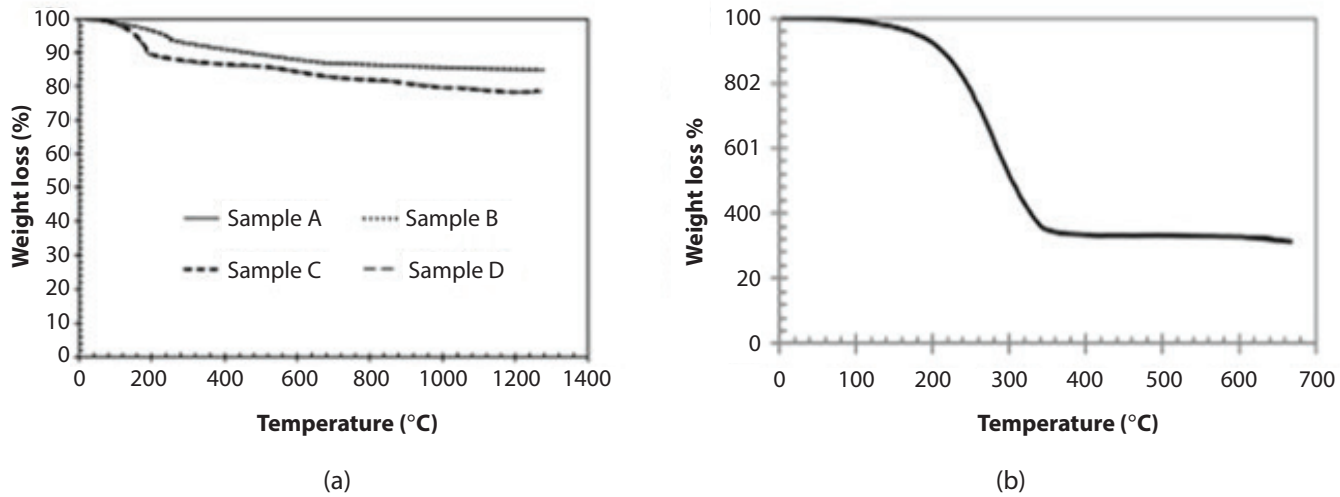

(a) (b)

Figure 11 Loss on ignition (a) produced samples A, B, C and D for a different formulation of brake pad materials and (b) commercial brake pad

thermal stability – an indication of good resistance to thermal decomposition.

Thermal Conductivity

Braking efficiency is a function of the thermal conductivity of brake pads. Thus, an increase in the thermal conductivity of brake pads causes an increase in brake efficiency. This is because the heat generated during braking can easily be absorbed and dissipated. However, when the thermal conductivity of a brake pad is extremely high, this may lead to deterioration of the hydraulic fluid and may affect the engineperformance [9]. The generally acceptable range of thermal conductivity of a brake pad is 0.407 – 0.804 W/mK [15]. Tables 4 and 5 show the thermal analysis results of the commercial brake pad and samples produced, respectively. Table 4 shows the thermal conductivity of the commercial brake pad, while Table 5 shows the results of thermal conductivities of the experimental samples A to D produced at different temperatures. The thermal conductivity of the samples ranges between 134 and 193 W/mK, which is quite high compared to the standard. The samples thermal conductivity decreased significantly with an increase in temperature. The higher thermal conductivities obtained for the produced samples are connected to higher percent proportions of heat conductivity (metallic) elements such as aluminium, manganese and iron present in the chemical composition of the steel slag, as shown in Table 3. The decrease in thermal conductivity of the samples could be due to these elements' fast dissipation of heat.

Table 4 Thermal conductivity analysis of the commercial brake pad

Thickness (mm)	Thermal conductivity (W/mK)	Coefficient of friction (%)	Roughness (Ra)
5.20	0.2550	0.55	3.50

Table 5 Thermal conductivity analysis of experimental samples A to D (W/mK)

Sample	Temp (50 °C)	Temp (100 °C)	Temp (170 °C)	Temp (200 °C)	Temp (250 °C)	Temp (300 °C)
A	193.5	186.5	187.4	155.2	156.4	150.4
B	190.7	182.4	174.3	154.6	142.3	143.2
C	187.8	183.3	175.6	145.5	133.6	137.5
D	190.8	184.7	180.6	152.5	144.5	135.7

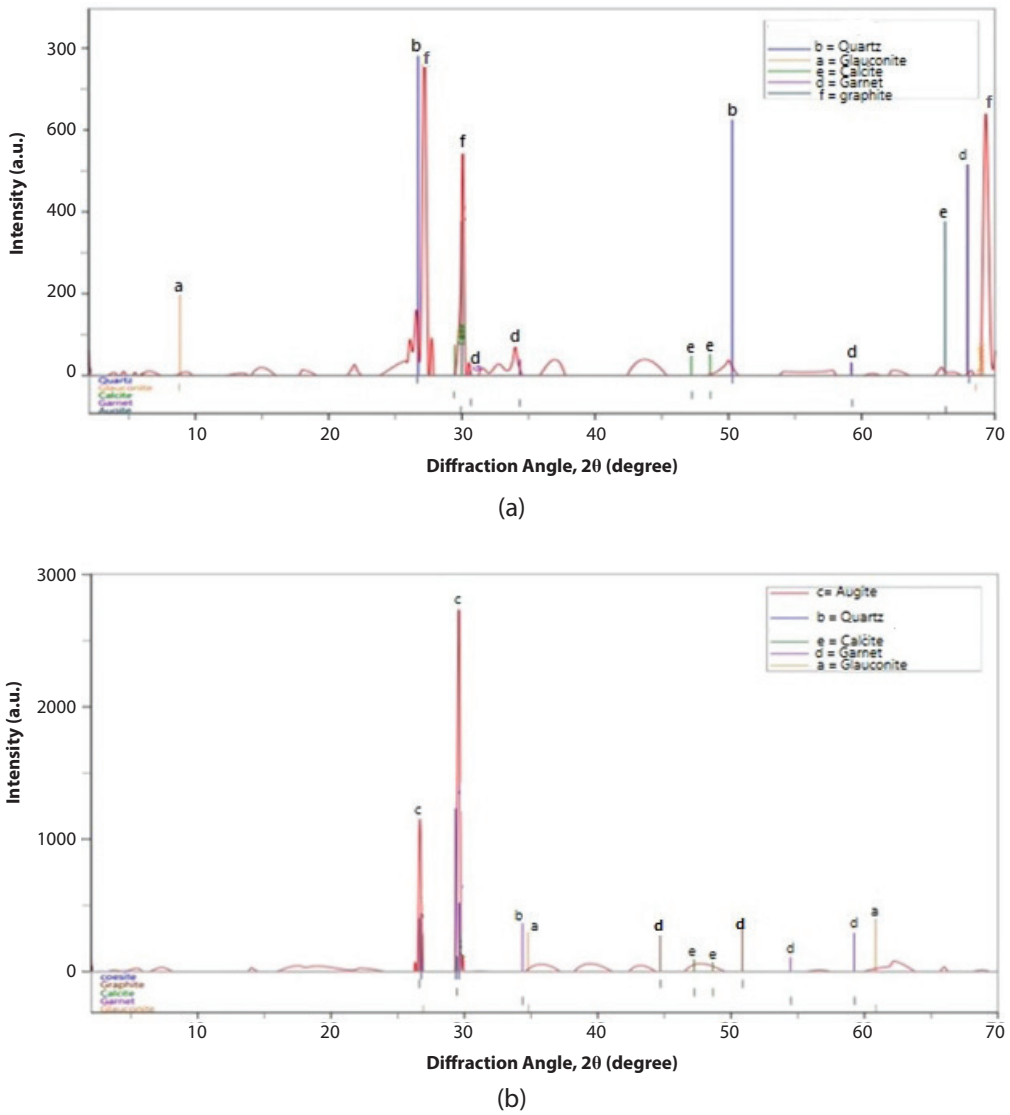

Figure 12 X-ray diffraction analysis of the (a) experimental sample A (b) commercial brake pad

Structural Analysis of the Samples

Figure 12 shows the X-Ray Diffractions of experimental sample A, and commercial brake pad plotted for the intensity of X-rays scattered at different angles. Similar plots were obtained for samples B, C and D. The details of the phases obtained are presented in Table 6. The table shows that the phases present in samples A to D and the commercial brake pad are similar except for the augite phase, which is absent in the experimental samples. Graphite is also absent in the commercial brake pad.

Figure 13 shows the Scanning Electron Micrographs (SEM) of samples A, B, C and D produced with different proportions of materials investigated. As shown in Figure 13a, the silica, steel slag and phenolic resin are more visible in sample A. While some materials such as $CaCO_3$ and silica are more pronounced in volume fraction, steel slag and phenolic resin proportions are scanty. Furthermore, there is a coalescence of $CaCO_3$ in sample A with a lower proportion of phenolic resin. However, Figure 13d indicates adequate dispersion with or no coalescence of $CaCO_3$ when phenolic resin and steel slag were added. It also appears that $CaCO_3$ is well dispersed in Figure 13d. The addition of steel slag, silica and $CaCO_3$ altered the usual endothermic and exothermic reactions and chemical structure where there are chemical reactions. This is because the reaction is complex when these materials are added to the resin. Generally, the curing process with phenolic resin is temperature-dependent and dehydration – condensation reaction started and

Table 6 XRD results of the commercial brake pad and produced brake pads of samples A to D

Phase	Formula	Sample A (K*)	Sample B (K*)	Sample C (K*)	Sample D (K*)	Control sample (K*)
Coesite/Quartz	SiO_2	0.766	0.844	2.754	1.370	1.889
Graphite/graphite-2H	C	1.241	3.023	1.632	0.682	-
Calcite	$CaCO_3$	1.427	1.353	1.520	0.420	2.106
Garnet	3 (Ca.Fe.Mg)O. (Al.Fe)	2.850	2.023	2.911	2.938	3.330
Glauconite	(K.CaO.Na)	2.770	1.955	3.079	1.581	3.066
Augite	N(CaO.(Mg.Fe) O.Si	-	-	-	-	1.539

(K*) is the figure of merit of the samples.

ended at 90°C and 250°C, respectively. At higher temperatures, there was an easy flow of the molten resin, which caused an improvement in the cross-link of molecules and consequently an improvement of binder bonding strength. This study has shown that the addition of silica and $CaCO_3$ affected the binding properties of phenolic resin, while steel slag seems to exhibit a lesser effect [23].

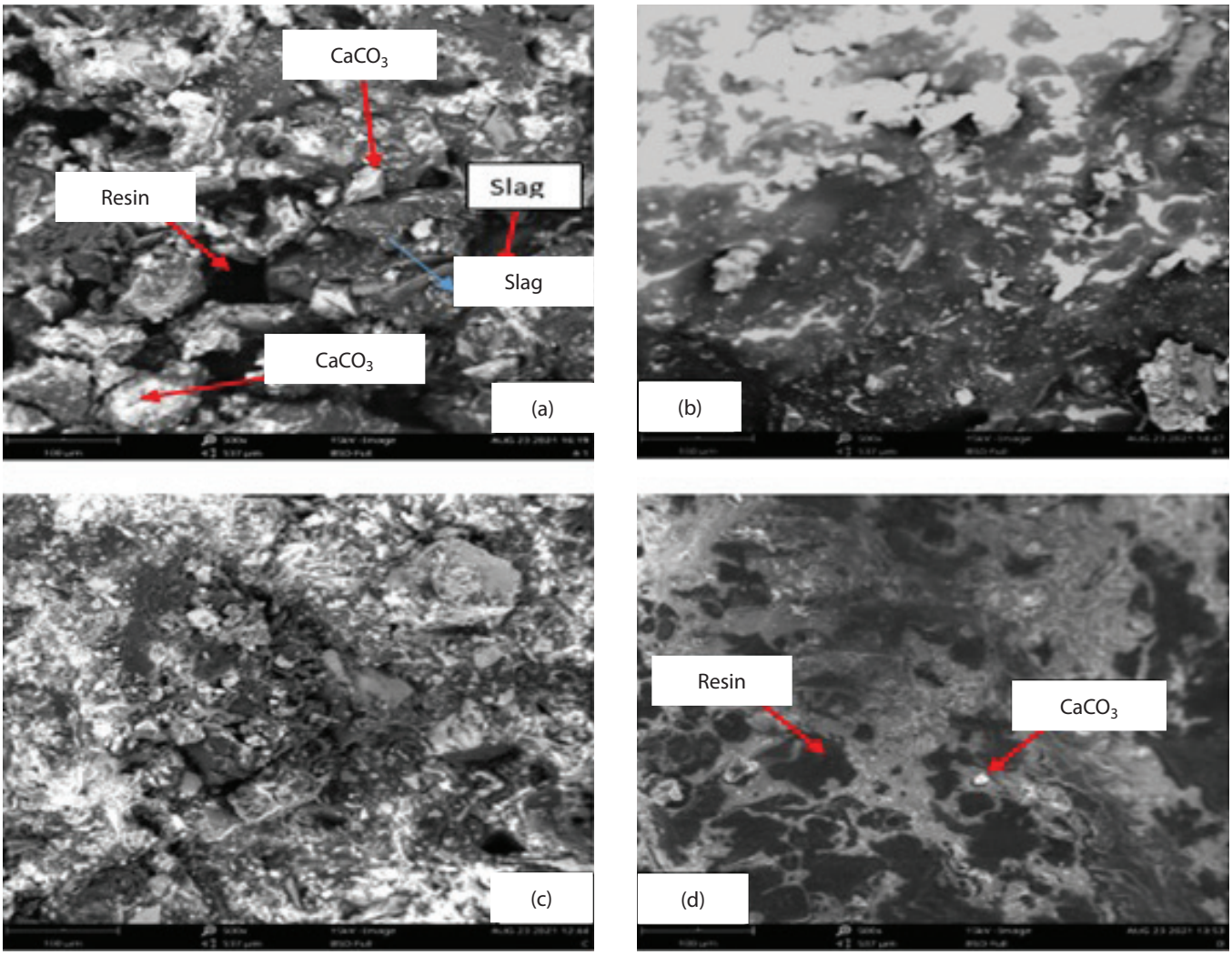

Figure 13 Scanning electron micrographs (SEM) of the produced brake pad (a) Sample A, (b) Sample B, (c) Sample C and (d) Sample D

CONCLUSIONS

This study investigated the physical, mechanical, chemical, thermal and tribological characteristics of non-asbestos brake pads in the form of hybrid-polymer matrix composites by stir casting method using steel slag, silica, calcium tri-oxocarbonate IV and graphite, and phenolic resin as input materials in varying weight percentages. The control sample exhibited the lowest wear rate of 0.6 and 0.8 g/Nm at loads of 7.5 and 10 N, respectively. This implies better wear resistance characteristics than the other sample. The samples exhibited appreciably high coefficient of friction of 0.410, 0.413, 0.440 and 0.40 for samples A, B. C and D, respectively, which is within the acceptable limit (0.3 – 0.6) for the brake pad. Sample A exhibited the highest compressive strength of 7.78 MPa, which is followed by samples C (3.04 MPa) and D (1.52 MPa). The results suggest that the compressibility of samples decreased with increasing steel slag and phenolic resin content. Sample D, which exhibited a lower wear rate (1 g/Nm) and coefficient of friction (0.40) than samples A, B, and C, exhibited the lowest water absorption rate, which could be attributed to the increase in density of sample D. The specific gravity of the samples produced ranges between 2.45 and 2.61, which agrees with the values of 2.27 – 3.25 reported in works of literature and compare well with the commercial brake pad. Sample A was produced with the lowest proportion of steel slag and phenolic resin and exhibited the lowest acetone extraction, which could be because of the higher per cent proportion of steel slag and, more importantly, the phenolic resin that experienced chemical reaction. Samples A and B exhibited better thermal stability – an indication of good resistance to thermal decomposition. The thermal conductivity of the samples ranges between 137 and 193 W/mK, which is quite high compared to the standard. The thermal conductivity of the samples decreased significantly with an increase in temperature. The high thermal conductivities obtained for the samples are due to high per cent proportions of heat conductivity (metallic) elements such as aluminium, manganese, and iron present in the steel slag. X-ray diffraction results revealed that similar phases are present in the samples and commercial brake pad except for the graphite-2H present, which was found in the experiment samples, and augite was available in the commercial brake pad. The microstructure showed a fair distribution of the proportion of the constituents in phenolic resin, which enhanced its binding property and ultimately enhanced the properties of the samples.

REFERENCES

[1] M.A. Maleque & U. Abdullahi, "Materials and processing route for aircraft brake system", *International Journal of Mechanical and Materials Engineering (IJMME)*, 8, 1, pp. 14- 20, 2013.

[2] Z.U. Elakhame, O.J. Omowunmi, A.O. Komolafe, O.O. Olotu, P.O. Kaffo, N.A. Alausa, Y.J. Obe & A.A. Ojuolape, "Manufacture of automotive brake pads from sawdust composites", *International Journal of Scientific & Engineering Research*, 8, 8, pp. 1228-1234, 2017.

[3] S.S. Lawal, N.A. Ademoh, K.C. Bala & A.A. Salawu, "Production and testing of brake pad composites made from cashew nut shells and plant gum binder", *Journal of the Nigerian Institution of Mechanical Engineers*, 9, 2, pp. 54-63, 2019.

[4] S.I. Durowaye, O.I. Sekunowo & G.I. Lawal, "Thermal and tribological characterisation of asbestos-free particulate ceramic matrix composites", *Kufa Journal of Engineering*, 11, 2, pp. 49- 66, 2020.

[5] N.A. Ademoh & I.A. Olabisi, "Development and evaluation of smaise husk (asbestos-free) based pad", *Industrial Engineering Letters*, 5, 2, pp. 67-80, 2015.

[6] R. Vijay, J.M. Jees, M.A. Saibalaji & V. Thiyagarajan, "Optimisation of tribological properties of non-asbestos brake pad material by using steel wool", *Hindawi Publishing Corporation. Advances in Tribology*, pp. 1-10, 2013.

[7] A.L. Cracium, C. Pinca-bretotean, C. Birtok-baneasa & A. Josan, "Composite materials for friction and braking application", *Institute of Physics (IOP) Publishing*, *IOP Conference Series: Materials Science and Engineering*, 200, pp. 1-10, 2017.

[8] S. Durowaye, B. Bolasodun, W. Ayoola, A. Olarinde & Q. Apena, "Improvement of polyethylene matrix composites using coconut shell and cow bone particulates", *Kufa Journal of Engineering*, 10, 3, pp. 134-150, 2019.

[9] G. Akincioglu, H. Oktem, I. Uygur & S. Akincioglu, "Determination of friction-wear performance and properties of eco-friendly brake pads reinforced with

hazelnut shell and boron dusts", *Arabian Journal for Science and Engineering*, 43, 9, pp. 4727-4737, 2018.

[10] I. Mutlu, I. Sugozu & A. Keskin, "The effects of porosity in friction performance of brake pad using tire dust", *Polimeros*, 25, 5, pp. 440-446, 2015.

[11] R.A. Tatara, S. Suraparaju & K.A. Rosentrator, "Compression molding of phenolic resin and corn-based DDGS blends", *Journal of Polymers and the Environment,* 15, 2, pp. 89-95, 2007.

[12] M. Erikssona, J. Lord & S. Jacobson, "Wear and contact conditions of brake pads: dynamical in situ studies of pad on glass", *Wear,* 249, 3-4, pp. 272-278, 2001.

[13] K.K. Ikpambese, D.T. Gundu & L.T. Tuleun, "Evaluation of palm kernel fibers (PKFs) for production of asbestos-free automotive brake pads", *Journal of King Saud University – Engineering Sciences*, 28, pp. 110-118, 2016.

[14] S. Zhang, Q. Hao, Y. Liu, L. Jin, F. Ma, Z. Sha & D. Yang, "Simulation study on friction and wear law of brake pad in high-power disc brake", *Mathematical Problems in Engineering*, pp. 1-15, 2019.

[15] A.O.A. Ibhadode & I.M. Dagwa, "Development of asbestos-free friction lining material from palm kernel shell", *Journal of the Brazil Society of Mechanical Science and Engineering*, 30, 2, pp. 166-173, 2008.

[16] H.R. Akramifard & Z. Ghasemi, "Friction and wear properties of a new semi-metallic brake pad according to SAE J 661: a case study in pars lent complex (Iran)", *International Journal of New Technology and Research (IJNTR)*, 2, 3, pp. 96-99, 2016.

[17] M. Unaldi & R. Kus, "The determination of the effect of mixture proportions and production parameters on density and porosity features of miscanthus reinforced brake pads by taguchi method", *International Journal of Automotive Engineering and Technologies*, 7, 1,pp. 48-57, 2018.

[18] T.R. Jaafar, M.S. Selamat & R. Kasiran, "Selection of best formulation for semi- metallic brake friction materials development. *Powder Metallurgy*, pp. 1-30, 2012.

[19] Z.U. Elakhame, "Development and production of brake pads from palm kernel shell composites", *International Journal of Scientific and Engineering Research,* 5, 10, pp. 734- 744, 2014.

[20] J. B. Baruah, A. Saikia, J. C. Sarma, J. G. Handique, B. Sarma, R. J. Sarma, A. J. Thakur, A. Puzari, P. K. Bhattacharyya, S. Padhye, M. D. Saikia, P. Gogoi, S. Hazarika, N. N. Dutta, V. J. Mayani, B. Mondal, N. C. Barua, & P. P. Saikia, "Chemistry of phenolic compounds: state of the art", Editor: J.B. Baruah, *Nova Science Publishers*, 2011.

[21] A. Knop & L.A. Pilato, "Degradation of phenolic resins by heat, oxygen and high energy radiation", *Phenolic resin, Springer-Verlag*, Berlin Heidelberg, pp. 140-146, 1985.

[22] R. Yun, P. Filip & Y. Lu, "Performance and evaluation of eco-friendly brake friction materials", *Tribology International*, 43, 11, pp. 2010-2019, 2010.

[23] J. Zhang, G. Mei & S. Zhao, "Curing mechanism of phenolic resin binder for oxide-carbon refractories", *Iron and Steel Institute of Japan (ISIJ) International*, 56, 1, pp. 44-49, 2016.